Structures and Properties of *N*-Methyltetraphenylporphyrin Complexes. The Crystal and Molecular Structure of Chloro-*N*-methyl-α,β,γ,δ-tetraphenylporphinatozinc(II) and the Chelate Effect of Zn(II), Co(II), and Cd(II) *N*-Methylporphyrin Complexes

David K. Lavallee,*[1] Alan B. Kopelove, and Oren P. Anderson*

Contribution from the Department of Chemistry, Colorado State University, Fort Collins, Colorado 80523. *Received September 1, 1977*

Abstract: The crystal and molecular structure of chloro-*N*-methyl-α,β,γ,δ-tetraphenylporphinatozinc(II), $Zn(N_4C_{45}H_{31})Cl \cdot \frac{2}{3}CH_2Cl_2$, has been determined from three-dimensional single-crystal x-ray diffraction data, collected by counter techniques. The dark purple crystals are triclinic, space group $P\bar{1}$ (No. 2), with two formula units in a unit cell of dimensions $a = 11.970$ (6) Å, $b = 13.468$ (8) Å, $c = 14.998$ (7) Å, $\alpha = 101.73$ (1)°, $\beta = 107.00$ (2)°, and $\gamma = 115.88$ (2)°. The structure, which includes two-thirds of a molecule of dichloromethane (on the average) in the asymmetric unit, has been refined by least-squares methods to $R = 0.069$ ($R_w = 0.076$) for 3302 unique reflections with $F^2 > 3\sigma(F^2)$. The zinc(II) ion of the monomeric neutral complex is strongly bound to only three of the pyrrole nitrogen atoms of the *N*-methylporphyrin ligand (Zn-N = 2.018 (9), 2.081 (9), and 2.089 (6) Å). A very long distance (Zn-N = 2.530 (7) Å) is observed between the zinc(II) ion and the alkylated pyrrole nitrogen. The chloride ion is strongly bound to zinc (Zn-Cl = 2.234 (3) Å) in a position above the mean metal-*N*-methylporphyrin plane, while the *N*-methyl group occupies a position below the metal ion. The zinc ion is displaced by 0.65 Å from the plane of the three strongly bound pyrrole nitrogen atoms. Despite the large displacement of the Zn(II) atom from the plane of the complexing nitrogen atoms, the *N*-methylporphyrin ligand exhibits the kinetic chelate effect, with no displacement of the metal atom observed after 1 week at 25 °C with 1.0 M di-*n*-butylamine or 1.0 M diethylamine in DMF or 1.6 M acetylacetone in CH_3CN. Similar results are obtained for the normally labile ions Co(II) and Cd(II) as chloro-*N*-methyltetraphenylporphyrin complexes. The chloro-*N*-methyltetraphenylporphyrin complexes of these ions do not exchange metal atoms with *N*-methyldeuteroporphyrin IX dimethyl ester over a period of 1 week. This observation and the lack of exchange of Cd(II) from chloro-*N*-methyltetraphenylporphyrin in diethylamine demonstrate that replacement of Cd(II) by Cu(II) is not due to simple dissociation of the cadmium *N*-methylporphyrin complex. Kinetic studies show, however, first-order dependence of the replacement rate on water concentration and catalysis of the metal exchange reaction by Ni^{2+}, supporting a mechanism in which the cadmium *N*-methylporphyrin complex undergoes acid-assisted dissociation before the formation of the copper complex. There is no compelling evidence to support the associative electrophilic cis (same side) attack mechanism that has been proposed for the replacement of Cd(II) in chloro-*N*-methyltetraphenylporphinatocadmium(II) by Cu(II).

The nonalkylated porphyrin ligand system exhibits a pronounced kinetic chelate effect. Rates of exchange of a metal ion from one porphyrin to another are generally very slow. Thus, Fe(III) protoporphyrin does not readily transfer Fe(III) to tetraphenylporphyrin,[2a] nor does Mg(II) chlorophyll a transfer Mg(II) to chlorophyll b.[2b] Similarly, metal ion replacement rates, which depend to a large extent on the stability of the metalloporphyrin reactant,[3] are very slow (≫1 day at 25 °C) for Co(II) in solution replacing Co(II) in mesoporphyrin[4] or for Cu(II) replacing Zn(II) in tetraphenylporphyrin.[3]

In view of the large out-of-plane displacement of the metal atom in *N*-methylporphyrin complexes, herein reported for Zn(II) and previously reported for Co(II)[5] and Mn(II),[6] it is of interest to determine whether the *N*-methylporphyrin ligand system exhibits a kinetic chelate effect, such as that found for nonmethylated porphyrins. In view of recent work on the mechanism of replacement of Cd(II) in Cd(*N*-CH_3TPP)Cl (H*N*-CH_3TPP = *N*-methyl-α,β,γ,δ-tetraphenylporphyrin) by copper(II),[7] the results of studies of metal ion exchange reactions which shed light on the mechanism of such metal replacement reactions would seem to be of interest. Finally, a study of the structure of the Zn(*N*-CH_3TPP)Cl complex was undertaken to discover the effects of incorporating a d^{10} metal ion with a strong preference for four-coordination into the highly distorted and relatively rigid coordination environment provided by the *N*-CH_3TPP ligand system.

Experimental Section

Synthesis of Complexes. Synthesis of the *N*-methyl-α,β,γ,δ-tetraphenylporphyrin (H*N*-CH_3TPP) from tetraphenylporphyrin and CH_3SO_3F under dilute conditions has been described previously.[8] The synthesis of chloro-*N*-methyltetraphenylporphinatozinc(II) and chloro-*N*-methyltetraphenylporphinatocobalt(II) (by addition of an excess of the hydrated chloride salts in acetonitrile to H*N*-CH_3TPP in dichloromethane, addition of noncoordinating base (2,6-lutidine), and multiple recrystallization from CH_3CN/CH_2Cl_2 solutions) has also been described.[9] The analysis of the Zn(II) complex (Anal. Calcd for $ZnC_{45}H_{31}N_4Cl$: C, 74.17; H, 4.29; N, 7.69. Found: C, 74.05; H, 4.39; N, 7.55) shows that the bulk of the material contains no solvent of crystallization following drying for 1 h at 100 °C (see below). Cd(*N*-CH_3TPP)Cl was synthesized from a slurry of $CdCl_2$ in methanol to which H*N*-CH_3TPP dissolved in dichloromethane was added slowly. Excess $CdCl_2$ was filtered off and the solution taken to dryness. The solid was dissolved in dichloromethane and crystallized from 1:1 v/v CH_3CN/CH_2Cl_2. Dissolution of the crystals and recrystallization from CH_3CN/CH_2Cl_2 solution was repeated twice, giving dark purple needlelike crystals. The visible spectrum is much like that of Zn(*N*-CH_3TPP)Cl, showing a split Soret band and having the following molar absorptivities (M^{-1} cm^{-1}) at the indicated wavelengths of maximum absorption: 667 nm, 9.62×10^3; 620 nm, 1.44×10^4; 568 nm, 8.15×10^3; 452 nm, 2.15×10^5; and 443 nm, 2.77×10^5. Absence of H*N*-CH_3TPP was verified by lack of its characteristic peaks in the visible absorption spectrum[8] and absence of protonated H*N*-CH_3TPP was shown by lack of any change in the visible absorption spectrum upon addition of the noncoordinating base 2,2,6,6-tetramethylpiperidine. Attempts to crystallize salts of Cd*N*-CH_3TPP$^+$ with the noncoordinating counterion $CF_3SO_3^-$ were unsuccessful.

Solvents and amines were distilled and dried by typical procedures.[10] The water content of the distilled dimethylformamide used for kinetic studies was determined to be 0.02% by gas chromatographic analysis. Water was twice distilled, the second time from alkaline permanganate solution. Tetra-*n*-butylammonium tetrafluoroborate (Southwestern Analytical Chemicals, Inc., electrochemical grade) was dried 1 h at 100 °C and used without further purification. Copper tetrafluoroborate (Alfa Ventron) was dried over $CaCO_3$ and the stock

0002-7863/78/1500-3025$01.00/0

Table I. Atomic Coordinates (Fractional)[a]

Atom	x	y	z
Zn(II)	−0.19662 (10)	0.08278 (9)	0.12969 (7)
N-1	−0.3353 (6)	−0.1249 (5)	0.1256 (5)
N-2	−0.2687 (6)	−0.0207 (6)	−0.0218 (5)
N-3	−0.2647 (6)	0.1189 (6)	0.2378 (5)
N-4	−0.2085 (6)	0.2130 (6)	0.0890 (5)
Cl^-	0.0071 (2)	0.1075 (2)	0.2145 (2)
C-5	−0.4702 (8)	−0.1393 (7)	0.0709 (6)
C-11	−0.3015 (8)	−0.1994 (7)	0.0750 (6)
C-12	−0.2467 (9)	−0.2420 (8)	0.1457 (7)
C-13	−0.2433 (8)	−0.1915 (8)	0.2345 (6)
C-14	−0.2967 (8)	−0.1176 (7)	0.2252 (6)
C-21	−0.2606 (8)	0.0291 (7)	−0.0947 (6)
C-22	−0.2942 (10)	−0.0580 (8)	−0.1859 (6)
C-23	−0.3189 (10)	−0.1585 (8)	−0.1700 (7)
C-24	−0.3008 (8)	−0.1357 (7)	−0.0681 (6)
C-31	−0.2948 (8)	0.0645 (7)	0.3031 (6)
C-32	−0.3145 (9)	0.1340 (7)	0.3762 (6)
C-33	−0.2921 (9)	0.2323 (7)	0.3579 (6)
C-34	−0.2580 (8)	0.2256 (7)	0.2727 (6)
C-41	−0.1983 (8)	0.3100 (7)	0.1492 (6)
C-42	−0.1685 (9)	0.3985 (7)	0.1045 (7)
C-43	−0.1665 (9)	0.3518 (7)	0.0178 (7)
C-44	−0.1924 (8)	0.2348 (7)	0.0065 (6)
C-1	−0.2972 (8)	−0.0417 (6)	0.3026 (6)
C-2	−0.2195 (8)	0.3182 (7)	0.2356 (6)
C-3	−0.2185 (7)	0.1490 (7)	−0.0789 (5)
C-4	−0.3053 (8)	−0.2172 (7)	−0.0200 (6)
Cl-1 (9.2 (2))	−0.4136 (6)	0.5659 (5)	−0.3738 (4)
Cl-2 (9.4 (2))	−0.2514 (6)	0.4687 (5)	−0.4047 (4)
C-99 (5.3 (3))	−0.2706 (15)	0.5927 (13)	−0.3939 (11)
H-12	−0.2172	−0.2963	0.1321
H-13	−0.2097	−0.2033	0.2948
H-22	−0.2985	−0.0465	−0.2470
H-23	−0.3432	−0.2319	−0.2186
H-32	−0.3386	0.1137	0.4278
H-33	−0.2981	0.2954	0.3940
H-42	−0.1531	0.4759	0.1323
H-43	−0.1507	0.3898	−0.0279
H-1-C-5	−0.4636	−0.0648	0.0947
H-2-C-5	−0.4938	−0.1636	0.0005
H-3-C-5	−0.5385	−0.1978	0.0826

[a] Estimated standard deviations in parentheses. For the solvent atoms, the isotropic thermal parameter B (from the expression $\exp(-B(\sin^2\theta/\lambda^2))$) is given in parentheses immediately following the atom name.

solutions standardized spectrophotometrically with EDTA. Nickel trifluoromethanesulfonate was made from $NiCO_3$ and HCF_3SO_3 (3M Co., distilled in an all-glass apparatus) and tetra-*n*-butylammonium trifluoromethanesulfonate was made by the neutralization of an aqueous solution of tetra-*n*-butylammonium hydroxide with HCF_3SO_3. Both salts were crystallized, washed thoroughly with anhydrous ether, and dried under vacuum.

Kinetic experiments on the replacement of Cd(II) in Cd(*N*-CH_3TPP)Cl by Cu^{2+} utilized the Soret region (400–500 nm) and isosbestic points were observed at 436 and 468 nm in the presence and in the absence of added water. The product was identified by its absorption spectrum[11] and rate of demethylation with di-*n*-butylamine.[12,13]

Instrumentation. Visible absorption spectra were obtained on a Cary 14 spectrophotometer thermostated with a Haake FK-2 circulating bath. An Enraf-Nonius CAD-3 diffractometer was employed for crystal data collection. A Varian Aerograph gas chromatograph with Porapak Q column was used for water content analysis.

Crystal Data. For $Zn(N_4C_{45}H_{31})Cl\cdot\frac{2}{3}(CH_2Cl_2)$ (see below): fw 785.22; triclinic; a = 11.970 (6) Å; b = 13.468 (8) Å; c = 14.998 (7) Å; α = 101.73 (1)°; β = 107.00 (2)°; γ = 115.88 (2)°; V = 1920.4 Å^3; ρ_{calcd} = 1.36 g cm^{-3}; Z = 2; $F(000)$ = 808; space group $P\bar{1}$; Mo Kα radiation; λ_1 = 0.70930 Å; λ_2 = 0.71359 Å; μ(Mo Kα) = 8.60 cm^{-1}.

Data Collection and Reduction. The dark purple crystals first examined by Weissenberg and precession photography were revealed to be isomorphous with the corresponding chlorocobalt(II)[5] and chloromanganese(II)[6] derivatives of the *N*-CH_3TPP ligand. Crystals of this habit were invariably twinned, however, and unsuitable for data collection. Diligent search revealed a *very* small minority of crystals which had crystallized with a different external habit. Preliminary x-ray photography of crystals of this second habit revealed a tendency to be relatively highly mosaic (presumably due to slow loss of solvent of crystallization, see below), but a crystal suitable for data collection was eventually found. Preliminary photography on this crystal revealed only Laue symmetry $\bar{1}$, consistent with the space groups $P1$ and $P\bar{1}$.[14] The centric space group $P\bar{1}$ was chosen arbitrarily for all further structural work with this compound. The correctness of this choice is attested to only by the ultimate solution and refinement of this structure, as reported below.

The crystal chosen for data collection was mounted on the Enraf-Nonius CAD-3 diffractometer, with the b axis approximately coincident with the diffractometer ϕ axis. After accurate centering, the orientation matrix for data collection and the unit cell parameters reported above were obtained from least-squares calculations on the automatically determined[15] 2θ, χ, and ϕ settings of 33 reflections (at ambient temperature, 20 (±1) °C) with 2θ values in the range 22–24°. No measured density was obtained, due to the difficulty in finding good crystals of the habit actually employed for data collection.

The intensity data were collected in two shells, the first with 4.5° $< \theta <$ 18°, and the second with 18° $< \theta <$ 25°. Solution and preliminary refinement of the structure were carried out on data from the low-θ shell (see below). The two shells taken together provided an intensity data base of 6546 unique reflections. The scan range employed was 0.5° (in θ) to either side of the calculated K$\bar{\alpha}$ peak position, at a constant scan rate of 10° min^{-1}. The number of times a given reflection was scanned varied according to the intensity, with weak reflections being scanned a maximum of four times. Background was

Table II. Anisotropic Thermal Parameters[a]

Atom	$10^4\beta_{11}$	$10^4\beta_{22}$	$10^4\beta_{33}$	$10^4\beta_{12}$	$10^4\beta_{13}$	$10^4\beta_{23}$
Zn(II)	88 (1)	65 (1)	48 (1)	45(1)	30 (1)	35 (1)
N-1	93 (9)	64 (6)	41 (4)	52 (6)	34 (5)	28 (4)
N-2	74 (8)	68 (7)	48 (5)	37 (6)	26 (5)	32 (5)
N-3	100 (9)	63 (6)	52 (5)	46 (7)	36 (6)	33 (5)
N-4	85 (9)	70 (7)	44 (5)	42 (7)	23 (5)	29 (5)
Cl^-	92 (3)	149 (3)	100 (2)	66 (3)	36 (2)	78 (2)
C-5	77 (10)	82 (9)	61 (6)	45 (8)	27 (7)	38 (6)
C-11	83 (11)	59 (8)	51 (6)	35 (7)	29 (6)	25 (6)
C-12	142 (14)	87 (9)	63 (7)	75 (10)	47 (8)	54 (7)
C-13	114 (12)	98 (9)	53 (6)	70 (9)	49 (7)	51 (7)
C-14	81 (10)	59 (7)	46 (6)	35 (7)	37 (6)	26 (5)
C-21	101 (11)	76 (8)	40 (5)	48 (8)	32 (6)	29 (6)
C-22	161 (14)	103 (10)	51 (6)	80 (10)	50 (8)	45 (7)
C-23	189 (15)	77 (9)	54 (7)	91 (10)	60 (8)	31 (7)
C-24	108 (11)	54 (8)	48 (6)	45 (8)	39 (7)	28 (6)
C-31	87 (11)	60 (8)	45 (6)	27 (8)	23 (7)	23 (6)
C-32	128 (12)	73 (9)	52 (6)	53 (9)	48 (7)	31 (6)
C-33	144 (13)	69 (8)	59 (6)	65 (9)	46 (8)	31 (6)
C-34	91 (11)	58 (8)	44 (6)	35 (8)	30 (6)	24 (5)
C-41	100 (11)	63 (8)	49 (6)	43 (8)	34 (7)	29 (6)
C-42	136 (14)	54 (8)	54 (7)	45 (9)	27 (8)	22 (6)
C-43	114 (12)	67 (9)	56 (7)	41 (9)	22 (7)	36 (6)
C-44	78 (10)	68 (8)	46 (5)	42 (8)	28 (6)	32 (6)
C-1	73 (10)	54 (7)	47 (5)	28 (7)	25 (6)	24 (5)
C-2	94 (11)	67 (8)	49 (5)	49 (8)	27 (6)	26 (6)
C-3	72 (10)	66 (8)	40 (5)	32 (7)	22 (6)	31 (5)
C-4	100 (11)	64 (8)	45 (6)	49 (8)	28 (6)	26 (6)

[a] Estimated standard deviations in parentheses. The form of the anisotropic thermal ellipsoid is given by: $\exp[-(\beta_{11}h^2 + \beta_{22}k^2 + \beta_{33}l^2 + 2\beta_{12}hk + 2\beta_{13}hl + 2\beta_{23}kl)]$.

Table III. Group Parameters for the Rigid Phenyl Rings[a]

Group	x_g[b]	y_g	z_g	δ[c]	ϵ	η
Ph-1	−0.2736 (4)	−0.1002 (4)	0.4798 (3)	−1.047 (4)	−2.923 (3)	1.047 (4)
Ph-2	−0.1944 (4)	0.5356 (3)	0.3465 (3)	−1.890 (3)	−2.817 (3)	2.549 (4)
Ph-3	−0.1906 (4)	0.2161 (3)	−0.2472 (3)	0.759 (6)	2.212 (4)	2.391 (6)
Ph-4	−0.2793 (4)	−0.4125 (3)	−0.1085 (3)	−1.153 (4)	2.633 (3)	−0.587 (4)

[a] Estimated standard deviations in parentheses. [b] x_g, y_g, and z_g are the fractional coordinates of the group centers. [c] The angles which describe the group orientations have been defined previously.[23]

counted at both ends of the scan, for a total time equal to the scan time. The takeoff angle was 3.5°, and zirconium foil attenuators were inserted automatically (to avoid coincidence losses) if the peak count rate exceeded 2500 counts s^{-1}. The intensity of one of three reference reflections ($00\bar{8}$, $60\bar{6}$, $\bar{2}4\bar{1}$) was measured every 25 reflections. None of these control reflections showed any significant or systematic changes in intensity during the course of data collection.

Lorentz and polarization corrections were applied to the observed data. The uncertainty parameter, g, in the formula used for the standard deviation in the intensity[16,17] was taken as 0.04. Reflections for which $F^2 > 3\sigma(F^2)$ were judged to be observed, and the 3302 reflections of the total merged data set which met this criterion were employed in the final refinement of the structure. No absorption correction was applied to the data, due to the low absorption coefficient ($\mu = 8.60$ cm^{-1} for Mo Kα radiation). The data collection crystal was a parallelepiped of approximate external dimensions 0.15 × 0.2 × 0.4 mm. Independent confirmation that the data collection crystal contained the desired Zn(N-CH_3TPP)Cl complex was obtained by x-ray fluorescence analysis on a single crystal with a diffraction pattern identical with the data crystal.[18]

Solution and Refinement of the Structure. The position of the zinc(II) ion was assigned from the highest nonorigin peak appearing in the Patterson map. Starting positions for all nonhydrogen atoms of the complex unit were then obtained from a series of Fourier syntheses phased by the atoms in known positions. Scattering factors for zinc, chlorine, carbon, and nitrogen were taken from ref 19. Scattering factors for spherical bonded hydrogen atoms[20] were also taken from ref 19, as were correction terms $\Delta f'$ and $\Delta f''$ for anomalous dispersion due to zinc and chlorine. Preliminary refinement of the positions and isotropic thermal parameters of the atoms of the *N*-CH_3TPP complex converged at a R ($= [\Sigma||F_o| - |F_c||]/\Sigma|F_o|$) value of 0.18 and a value of R_w ($= [\Sigma w(|F_o| - |F_c|)^2/\Sigma wF_o^2]^{1/2}$) of 0.23. The refinement at this stage was based on the 1847 observed reflections of the low-θ data shell (see above). At this point a difference Fourier synthesis revealed the presence of a partial molecule of dichloromethane within the asymmetric unit. Inclusion of this solvent molecule of crystallization resulted in an immediate and dramatic improvement in the above residual agreement indices.

Final least-squares refinement[21] of the structural model was carried out in alternate cycles on two separate blocks of parameters due to computer limitations. On cycle A, the scale factor was refined, together with the positional and anisotropic thermal parameters of zinc, the chloro ligand, the pyrrole nitrogens together with their C_α carbon atoms, and the *N*-methyl carbon. On each cycle B, the scale factor, the positional and anisotropic thermal parameters of the C_β carbons of the pyrrole rings and the meso carbon atoms, and the group positional and individual atomic isotropic thermal parameters of the phenyl rings were refined. The phenyl groups were refined as rigid, planar bodies of D_{6h} symmetry, with fixed C–C distances of 1.392 Å.[22,23] Hydrogen atoms (which were initially verified in a ΔF map) were included in fixed idealized positions 0.95 Å away from carbon, with isotropic thermal parameters 1 $Å^2$ larger than the carbon atom to which they were attached. The positions of the hydrogen atoms on C-5 (the *N*-methyl group) represent the results of a least-squares fit (idealized tetrahedral geometry) to the hydrogen atom positions observed about C-5 in a difference Fourier synthesis. The positional parameters, isotropic thermal parameters, and population parameters of the solvent molecule of crystallization were varied on both the A

Table IV. Derived Positional and Thermal Parameters for Phenyl Carbon and Hydrogen Atoms[a]

	Carbon				Hydrogen[b]		
Atom	x	y	z	B, Å^2	x_H	y_H	z_H
Ph-11	−0.2862 (6)	−0.0696 (5)	0.3957 (4)	3.4 (2)			
Ph-12	−0.3849 (5)	−0.1810 (4)	0.3866 (3)	3.7 (2)	−0.4673	−0.2489	0.3330
Ph-13	−0.3723 (6)	−0.2115 (4)	0.4707 (5)	4.7 (2)	−0.4249	−0.2799	0.4830
Ph-14	−0.2611 (6)	−0.1308 (6)	0.5639 (4)	4.9 (2)	−0.2951	−0.1868	0.5936
Ph-15	−0.1624 (5)	−0.0195 (5)	0.5730 (3)	6.3 (3)	−0.0798	0.0560	0.6132
Ph-16	−0.1749 (5)	0.0111 (4)	0.4889 (5)	5.1 (2)	−0.0975	0.0893	0.5128
Ph-21	−0.2075 (6)	0.4310 (4)	0.2921 (4)	3.2 (2)			
Ph-22	−0.892 (5)	0.5139 (5)	0.3810 (4)	3.7 (2)	−0.0177	0.4989	0.4046
Ph-32	−0.0761 (5)	0.6185 (4)	0.4353 (3)	4.4 (2)	0.0042	0.6747	0.4962
Ph-24	−0.1813 (6)	0.6401 (4)	0.4009 (4)	4.6 (2)	−0.0727	0.7112	0.4381
Ph-25	−0.2996 (5)	0.5572 (5)	0.3129 (5)	5.2 (2)	−0.3714	0.5720	0.2884
Ph-26	−0.3127 (5)	0.4527 (5)	0.2577 (4)	4.8 (2)	−0.3933	0.3962	0.1968
Ph-31	−0.2045 (6)	0.1847 (5)	−0.1665 (4)	3.3 (2)			
Ph-32	−0.0745 (5)	0.2466 (6)	−0.1640 (4)	5.7 (2)	0.0053	0.2674	−0.1073
Ph-33	−0.0607 (5)	0.2781 (6)	−0.2447 (5)	5.9 (2)	0.0284	0.3201	−0.2433
Ph-34	−0.1768 (7)	0.2476 (6)	−0.3280 (4)	4.5 (2)	−0.1670	0.2694	−0.3830
Ph-35	−0.3068 (5)	0.1857 (6)	−0.3305 (4)	5.6 (2)	−0.3855	0.1660	−0.3868
Ph-36	−0.3206 (5)	0.1542 (5)	−0.2498 (5)	5.0 (2)	−0.4086	0.1132	−0.2508
Ph-41	−0.2924 (6)	−0.3182 (4)	−0.0668 (4)	3.2 (2)			
Ph-42	−0.1866 (5)	−0.2971 (4)	−0.0962 (4)	3.9 (2)	−0.1232	−0.2184	−0.0877
Ph-43	−0.1736 (5)	−0.3914 (5)	−0.1378 (4)	4.7 (2)	−0.1018	−0.3773	−0.1581
Ph-44	−0.2662 (6)	−0.5069 (4)	−0.1502 (4)	4.9 (2)	−0.2785	−0.5832	−0.1763
Ph-45	−0.3719 (5)	−0.5279 (4)	−0.1208 (5)	5.1 (2)	−0.4213	−0.6115	−0.1364
Ph-46	−0.3850 (5)	−0.4336 (5)	−0.0791 (4)	4.2 (2)	−0.4464	−0.4258	−0.0541

[a] Estimated standard deviations in parentheses. [b] Fixed calculated positions, as described in the text. Each set of coordinates is that of a hydrogen atom attached to the phenyl carbon atom on the same line.

Table V. Bond Lengths (Angstroms) and Angles (Degrees) Involving Zn(II)[a]

	(a) Bond Lengths		
Zn(II)-N-1	2.530 (7)	Zn(II)-N-4	2.018 (9)
Zn(II)-N-2	2.089 (6)	Zn(II)-Cl$^-$	2.232 (3)
Zn(II)-N-3	2.081 (9)		
	(b) Bond Angles		
N-1-Zn-Cl$^-$	94.6 (2)	Zn-N-1-C-11	108.8 (5)
N-2-Zn-Cl$^-$	107.4 (2)	Zn-N-1-C-14	107.9 (4)
N-3-Zn-Cl$^-$	105.6 (2)	Zn-N-1-C-5	94.1 (5)
N-4-Zn-Cl$^-$	120.8 (2)	Zn-N-2-C-21	122.4 (5)
N-1-Zn-N-2	79.3 (3)	Zn-N-2-C-24	131.3 (6)
N-1-Zn-N-3	79.6 (3)	Zn-N-3-C-31	131.3 (7)
N-1-Zn-N-4	144.6 (2)	Zn-N-3-C-34	122.3 (6)
N-2-Zn-N-3	141.9 (2)	Zn-N-4-C-41	125.8 (6)
N-2-Zn-N-4	89.6 (3)	Zn-N-4-C-44	124.6 (7)
N-3-Zn-N-4	89.5 (3)		

[a] Estimated standard deviations in parentheses.

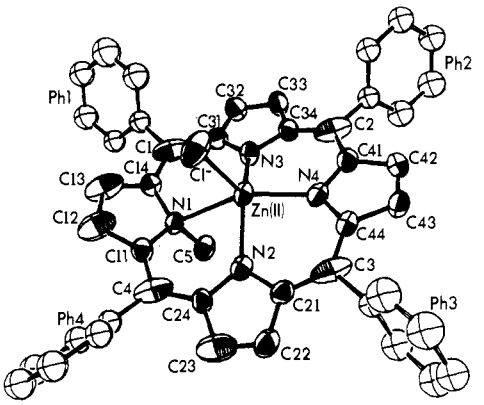

Figure 1. A view, in perspective, of the Zn(N-CH_3TPP)Cl complex. Hydrogen atoms have been omitted for clarity, and thermal ellipsoids are drawn at the 50% probability level.

and B cycles. With the population parameters of the carbon and chlorine atoms (hydrogen atoms of this moiety were not located) constrained to be equal, and with equal shifts applied to the population parameters of these three atoms, the value of the population parameter for this species (Cl-1, Cl-2, and C-99) converged to 0.670 (8) at the end of refinements (thus the chemical formula and formula weight given in the section on crystal data).

Several repetitions of this cycle A-B sequence of least-squares refinement (on F) lowered R to its final value of 0.069 (unobserved reflections not included) and R_w to 0.076. The error in an observation of unit weight was 1.87. On the final pair of refinement cycles, most shifts in parameter values were less than 20% of the estimated standard deviations in those parameters, with a few isolated cases of larger shifts (maximum was ~100% of the esd for two components of the anisotropic thermal ellipsoid for C-23). The NUCLS refinement program minimizes $\Sigma w(|F_o| - |F_c|)^2$, where F_o and F_c are the observed and calculated structure amplitudes, respectively, and w is the weight ($= 4F_o^2/\sigma^2(F_o^2)$) for each reflection. A final difference Fourier electron density map showed no peak higher than 0.52 e Å^{-3} and no depression lower than −0.43 e Å^{-3}.

Final atomic positional parameters for the nongroup atoms are listed in Table I. Table II lists the anisotropic thermal parameters obtained for the nongroup atoms. Table III contains the positional parameters for the rigid phenyl groups obtained directly from the refinement, while Table IV lists the positional parameters for the atoms of the rigid phenyl rings, as derived from the group orientations and geometries.

Structural Results and Discussion

The calculated bond lengths and angles involving Zn(II) in the chloro-N-methyl-$\alpha,\beta,\gamma,\delta$-tetraphenylporphinatozinc(II) complex (hereafter abbreviated as Zn(N-CH_3TPP)Cl) are reported in Table V, while the bond lengths and angles within the N-methyltetraphenylporphyrin ligand (hereafter N-CH_3TPP) are found in Table VI. In all cases, standard deviations reported include contributions from the errors in the unit cell parameters. Figure 1 shows the general layout of the complex and the numbering scheme employed in the following

Table VI. Bond Lengths (Angstroms) and Angles (Degrees) for the *N*-Methylporphyrin Ligand[a]

(a) Bond Lengths

N-1-C-5	1.48 (1)	N-3-C-31	1.38 (1)
N-1-C-11	1.40 (1)	N-3-C-34	1.38 (1)
N-1-C-14	1.40 (1)	C-31-C-32	1.43 (2)
C-11-C-12	1.43 (2)	C-32-C-33	1.34 (2)
C-12-C-13	1.35 (1)	C-33-C-34	1.45 (1)
C-13-C-14	1.41 (2)	C-31-C-1	1.42 (1)
C-11-C-4	1.38 (1)	C-34-C-2	1.42 (1)
C-14-C-1	1.38 (1)	N-4-C-41	1.36 (1)
N-2-C-21	1.40 (1)	N-4-C-44	1.37 (1)
N-2-C-24	1.38 (1)	C-41-C-42	1.45 (1)
C-21-C-22	1.42 (1)	C-42-C-43	1.34 (2)
C-22-C-23	1.34 (2)	C-43-C-44	1.43 (1)
C-23-C-24	1.43 (1)	C-41-C-2	1.38 (1)
C-21-C-3	1.41 (1)	C-44-C-3	1.39 (1)
C-24-C-4	1.42 (1)	C-1-Ph-11	1.50 (1)
		C-2-Ph-21	1.50 (1)
		C-3-Ph-31	1.52 (1)
		C-4-Ph-41	1.49 (1)

(b) Bond Angles

C-11-N-1-C-14	108.2 (8)	C-2-C-41-C-42	126.7 (9)
C-11-N-1-C-5	117.7 (6)	C-2-C-41-N-4	125.0 (9)
C-14-N-1-C-5	118.5 (8)	N-4-C-41-C-42	108.2 (8)
N-1-C-11-C-4	126.6 (9)	C-41-N-4-C-44	107.7 (8)
N-1-C-11-C-12	106.6 (8)	C-41-C-42-C-43	107.7 (9)
C-4-C-11-C-12	126.4 (10)	C-42-C-43-C-44	107.7 (9)
C-11-C-12-C-13	108.2 (11)	C-43-C-44-N-4	108.6 (8)
C-12-C-13-C-14	109.7 (9)	C-43-C-44-C-3	126.6 (9)
C-13-C-14-N-1	107.2 (8)	N-4-C-44-C-3	124.1 (8)
N-1-C-14-C-1	125.9 (9)	C-44-C-3-Ph-31	117.9 (8)
C-13-C-14-Cl	126.5 (8)	C-44-C-3-C-21	126.6 (9)
C-14-Cl-Ph-11	116.6 (8)	C-21-C-3-Ph-31	115.4 (7)
C-14-Cl-C-31	124.6 (9)	C-3-C-21-N-2	125.3 (7)
C-31-Cl-Ph-11	118.6 (7)	C-3-C-21-C-22	124.8 (9)
C-1-C-31-N-3	124.7 (9)	N-2-C-21-C-22	109.8 (8)
C-1-C-31-C-32	124.3 (9)	C-21-N-2-C-24	104.7 (7)
N-3-C-31-C-32	110.9 (9)	C-21-C-22-C-23	107.8 (9)
C-31-N-3-C-34	105.1 (8)	C-22-C-23-C-24	107.4 (9)
C-31-C-32-C-33	106.8 (9)	C-23-C-24-N-2	110.2 (9)
C-32-C-33-C-34	107.7 (10)	C-23-C-24-C-4	124.1 (9)
C-33-C-34-N-3	109.4 (8)	N-2-C-24-C-4	125.5 (8)
C-33-C-34-C-2	123.6 (9)	C-24-C-4-Ph-41	118.7 (8)
N-3-C-34-C-2	126.9 (9)	C-24-C-4-C-11	123.6 (9)
C-34-C-2-Ph-21	117.1 (8)	C-11-C-4-Ph-41	117.0 (8)
C-34-C-2-C-41	124.7 (9)		
C-41-C-2-Ph-21	118.2 (8)		

[a] Estimated standard deviations in parentheses.

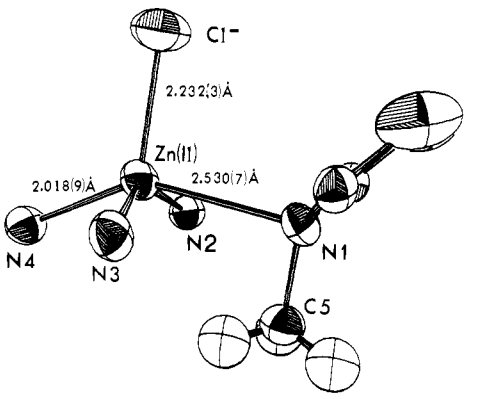

Figure 2. A view of the coordination geometry about the Zn(II) ion and the atoms of the N-1 pyrrole ring. A bond is shown between Zn(II) and N-1 to provide a convenient means of presenting the distance between these two atoms, although the interaction is very weak, at best (see discussion in text).

discussion, while Figure 2 provides a detailed view of the coordination geometry about the metal ion.

In discussing the detailed structure of the zinc(II) complex, and in comparing that structure with those of the previously established[5,6] structures of the cobalt(II) and manganese(II) complexes, the fact that zinc(II) is the smallest (in terms of ionic radius) of these three metal ions and that zinc(II) has the highest tendency toward four-coordination must be borne in mind. It is not surprising, therefore, to find that the interaction between the metal ion and the methylated pyrrole nitrogen atom, already weak in the Co(II) and Mn(II) complexes, is here lengthened (Zn-N-1 = 2.530 (7) Å) to the point where it becomes difficult to ascribe any bonding interaction to these two atoms. Attendant upon this further weakening are significant alterations in the ligand configuration, which will be commented upon below.

The other three pyrrole nitrogen atoms bind strongly to the metal ion. In agreement with our earlier studies, it is found that the pyrrole nitrogen atom trans to the N-methylated pyrrole ring forms the strongest bond to the metal ion (Zn-N-4 = 2.018 (9) Å), while the bonds to the other two pyrrole nitrogen atoms are somewhat longer (Zn-N-2 = 2.089 (6) Å, Zn-N-3 = 2.081 (9) Å). The shortest of these three bond lengths lies in the range reserved for four-coordinate (tetrahedral) zinc(II) complexes.[24] Indeed, noting the very long Zn-N-1 distance observed above, it is necessary to consider the zinc(II) ion in this structure to be essentially four-coordinate. The other two Zn-N (pyrrole) bond lengths are quite normal in length, compared to similar distances observed in other zinc-porphyrin complexes[25-27] and related compounds.[28] The zinc-chlorine bond length (Zn-Cl^- = 2.232 (3) Å) observed is consistent with the trend expected from our earlier studies,[5,6] and indicates strong binding of this ligand.

As has also been seen in our earlier studies of the cobalt(II) and manganese(II) *N*-CH_3TPP complexes, the zinc(II) ion is constrained to a position far above the mean plane of the *N*-CH_3TPP ligand. Adopting the plane of the three strongly bound pyrrole nitrogen atoms as a reference plane, zinc is found to be 0.65 Å above this plane, again reflecting the strong influence of the *N*-methyl group on the stereochemical binding properties of the *N*-methylporphyrin ligand. Corresponding displacements were 0.69 Å for the Mn(II) complex and 0.56 Å for the Co(II) species. This considerable displacement of the metal ion is, of course, reflected in the angles about zinc, and further corroboration of the essentially four-coordinate nature of the zinc(II) ion in this complex is provided by the extreme tilt of the chloro ligand toward the alkylated pyrrole nitrogen (as reflected in N-4-Zn-Cl^- of 120.8 (2)° vs. N-1-Zn-Cl^- of 94.6 (2)°). Although this tilt has been present in each of the *N*-CH_3TPP complexes we have studied, it reaches an extreme here in the Zn(II) complex along with the dramatic lengthening of the M-N-1 distance. It is difficult, however, to label the essentially four-coordinate geometry observed here as "pseudotetrahedral", as has been done for an earlier Co(II) complex of a related ligand,[29] especially in view of the N-4-Zn-N-2 and N-4-Zn-N-3 angles of essentially 90°, and we prefer to view the present structure as representing an extreme of distortion from an approximately square-based pyramid.

Much of the pattern of bonding and delocalization seen within the *N*-methylporphyrin ligand is very similar to that observed in the structures of the Co(II) and Mn(II) *N*-CH_3TPP complexes previously established. There are, however, some significant differences in conformation in the Zn(*N*-CH_3TPP)Cl complex which appear to be the result of the dramatic weakening of the interaction between the metal ion and the alkylated nitrogen atom. For example, the C_β-C_β (C-12-C-13) bond length in the alkylated pyrrole ring is observed to be 1.35 (1) Å, a value equal to the C_β-C_β bond lengths in the nonalkylated pyrrole rings and to the corre-

Table VII. Deviations From Least-Squares Planes[a]

(a) Plane 1
Atoms determining plane: N-1 (−0.427), N-2 (−0.136), N-3 (−0.17), N-4 (0.187), C-11 (−0.018), C-12 (0.700), C-13 (0.756), C-14 (0.075), C-21 (−0.238), C-22 (−0.534), C-23 (−0.579), C-24 (−0.309), C-31 (−0.137), C-32 (−0.366), C-33 (−0.343), C-34 (−0.098), C-41 (0.190), C-42 (0.272), C-43 (0.265), C-44 (0.203), C-1 (0.031), C-2 (0.073), C-3 (−0.013), C-4 (−0.145)
Other atoms: Zn^{2+} (0.594)

Plane 2
Atoms determining plane: N-2 (0.049), N-3 (0.086), N-4 (0.140), C-21 (−0.136), C-22 (−0.367), C-23 (−0.289), C-24 (−0.007), C-31 (0.047), C-32 (−0.249), C-33 (−0.346), C-34 (−0.112), C-41 (0.047), C-42 (0.014), C-43 (0.035), C-44 (0.105), C-1 (0.345), C-2 (−0.057), C-3 (−0.041), C-4 (0.272)
Other atoms: Zn^{2+} (0.724), N-1 (−0.082), C-11 (0.412), C-12 (1.222), C-13 (1.247), C-14 (0.456)

Plane 3
Atoms determining plane: N-2, N-3, N-4
Other atoms: Zn^{2+} (0.650), N-1 (−0.075)

Plane 4
Atoms determining plane: N-1 (−0.035), C-11 (0.002), C-12 (−0.006), C-13 (0.006), C-14 (−0.004)
Other atoms: Zn^{2+} (2.041), C-1 (0.139), C-4 (0.169)

Plane 5
Atoms determining plane: N-2 (−0.041), C-21 (0.000), C-22 (0.000), C-23 (0.000), C-24 (0.000)
Other atoms: Zn^{2+} (0.260), C-3 (0.096), C-4 (0.126)

Plane 6
Atoms determining plane: N-3 (−0.004), C-31 (0.019), C-32 (−0.009), C-33 (−0.003) C-34 (0.028)
Other atoms: Zn^{2+} (0.0298), C-1 (0.141), C-2 (0.124)

Plane 7
Atoms determining plane: N-4 (0.011), C-41 (−0.014), C-42 (0.013), C-43 (0.001), C-44 (−0.009)
Other atoms: Zn^{2+} (0.494), C-2 (−0.109), C-3 (−0.211)

Plane 8
Atoms determining plane: Ph-11-Ph-16
Other atoms: C-1 (0.087)

Plane 9
Atoms determining plane: Ph-21-Ph-26
Other atoms: C-2 (0.015)

Plane 10
Atoms determining plane: Ph-31-Ph-36
Other atoms: C-3 (−0.025)

Plane 11
Atoms determining plane: Ph-41-Ph-46
Other atoms: C-4 (−0.030)

(b) Equations of Planes[b]

Plane no.	*A*	*B*	*C*	*D*
1	10.032	−1.812	1.278	−2.550
2	10.324	−3.043	1.620	−2.796
3	10.420	−3.503	1.724	−2.765
4	7.595	4.984	−2.996	−3.511
5	11.153	−2.936	−1.316	−2.867
6	9.015	−1.369	3.350	−1.749
7	10.092	−2.298	1.593	−2.462
8	11.027	−9.366	−5.048	−4.501
9	−5.467	−6.026	12.907	2.308
10	−5.814	12.046	3.696	2.798
11	−4.174	4.603	−11.725	0.539

(c) Selected Dihedral Angles between Planes (deg)

3-1	7.4	3-7	5.3
3-2	2.0	2-8	50.3
3-4	38.5	2-9	74.7
3-5	11.6	2-10	85.2
3-6	12.3	2-11	45.4

[a] In section a, numbers in parentheses refer to the distance (angstroms) of the given atom from the calculated plane. [b] In the form $Ax + By + Cz = D$.

sponding distances in normal "planar"[30] porphyrins.[31] This is in strong contrast to the Co(II) and Mn(II) cases in which the metal-N-1 interaction was meaningful. In those cases the C_β-C_β bond length in the alkylated ring was observed to be ~1.39 Å, significantly longer than for the nonalkylated pyrrole rings. The C_α-C_β bond lengths observed here in the N-methylated pyrrole ring are longer than corresponding bond lengths in the Co(II) and Mn(II) *N*-CH_3TPP derivatives, and thus closer to the normal C_α-C_β bond lengths observed in the nonmethylated pyrrole rings. Thus, for the Zn(II) complex, the pattern of delocalization within the N-methylated pyrrole ring is much more like that found in a normal pyrrole ring of a nonalkylated porphyrin than like the patterns previously found in the corresponding portions of the N-methylated Co(II) and Mn(II) porphyrin complexes. The hybridization and resultant geometry at the N-methylated pyrrole nitrogen also reflect this change. The sum of the C-N-C angles about N-1 in the Zn(II) complex is ~344° (cf. 334° for the Co(II) derivative and 335° for the Mn(II) derivative), which is clear evidence for a strong shift toward trigonal, sp^2 nitrogen in the N-alkylated pyrrole in this complex, where no strong interaction with the metal ion exists. Finally, the tilt of the N-methylated pyrrole ring relative to the reference plane of the three nonmethylated pyrrole nitrogen atoms, clearly seen in

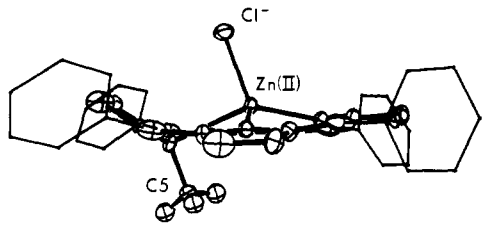

Figure 3. A side-on view of the Zn(*N*-CH_3TPP)Cl complex, showing the large out-of-plane displacement of the metal ion and the deviation of the N-methylated pyrrole ring from the mean plane of the remainder of the porphyrin core.

Figure 3 and tabulated in Table VII, is ~10° higher at 38.5° in the zinc(II) complex than was observed in the Co(II) and Mn(II) complexes, where interaction of the metal ions with N-1 did not allow such an extreme deviation in conformation to occur.

Thus, the size and strong tendency toward four-coordination of the zinc(II) ion have resulted in a *N*-CH_3TPP complex in which very little interaction is seen between the metal ion and the alkylated pyrrole nitrogen. It will be of interest to see how larger d^{10} metal ions (such as Cd(II) and Hg(II)) interact with the *N*-CH_3TPP ligand and make use of the relatively rigid coordination environment which it provides. An observation which may be related to the structure of these complexes is that the Soret band is noticeably split for the Zn(II) complex[11] and the Cd(II) complex (see the Experimental Section) but not for other complexes of *N*-CH_3TPP for which we have reported structures.[5,6,11]

Exchange Reactions

As is evident from the previous discussion, the metal ion is disposed well above the plane of complexing nitrogen atoms in *N*-methyltetraphenylporphyrin complexes. Unlike complexes of the non-N-methylated porphyrins, full coordination spheres of six ligands are not achieved in the *N*-methylporphyrin complexes. It is of interest, therefore, to determine whether the *N*-methylporphyrin ligand systems exert a significant chelate effect even with a low coordination number and distorted geometry. Two types of exchange reactions were investigated: transfer of the metal atom from one *N*-methylporphyrin to another and transfer of the metal atom to other ligands with a high affinity for the metal atom. The metal ions tested, Zn(II), Co(II), and Cd(II), are normally very labile to substitution. The exchange rate for dimethylformamide bound to Co(II) with bulk solvent molecules is 2.0×10^5 M^{-1} s^{-1}.[32] Although data are not available for DMF exchange for Zn(II) and Co(II), the rates can be estimated to be an order of magnitude slower than the exchange of bound water molecules to bulk solvent (from data for a number of ions in various solvents, compiled by Wilkins[33]), for which the rate constants are 3×10^7 and 4×10^8 M^{-1} s^{-1}, respectively.[34]

Metal atom exchange from one *N*-methylporphyrin to another was examined by the addition of a solution of the *N*CH_3TPP complex (Zn(II), Co(II), or Cd(II)) to a solution of *N*-methyldeuteroporphyrin IX dimethyl ester. The solvents employed (dichloromethane, acetonitrile, and dimethylformamide) were of varying polarity and metal complexing ability. The rates of exchange for these metal ions from one *N*-methylporphyrin to another are orders of magnitude slower than solvent exchange rates, as demonstrated by the fact that over a period of 1 week at 25 °C the spectrum of a solution of Co(*N*-CH_3TPP)Cl and *N*-methyldeuteroporphyrin IX dimethyl ester showed no noticeable change, being an additive spectrum of the two components (Figure 4). To ensure that a slow exchange rate rather than an unfavorable equilibrium constant is responsible for lack of exchange of Co(II) from the

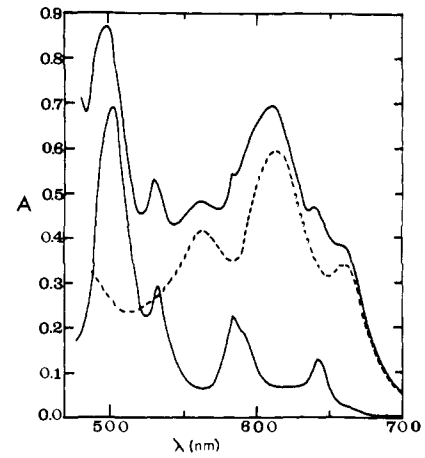

Figure 4. The lowest spectrum is that of *N*-methyldeuteroporphyrin IX dimethyl ester at 1.2×10^{-4} M. The dotted line is the spectrum of 1.2×10^{-4} M chloro-*N*-methyl-α,β,γ,δ-tetraphenylporphinatocobalt(II). The upper solid line spectrum is that due to a mixture of equal volumes of solutions of these two substances, each at 2.4×10^{-4} M before mixing. The solvent is dimethylformamide and the cell path length is 5 mm.

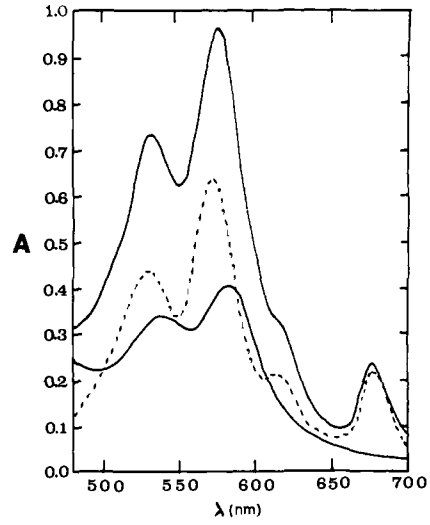

Figure 5. The lower solid line is the spectrum of a 1.0×10^{-4} M solution of chloro(*N*-methyldeuteroporphyrin IX dimethyl ester)cobalt(II). The dotted line is the spectrum of 1.0×10^{-4} M *N*-methyl-α,β,γ,δ-tetraphenylporphine. The upper solid spectrum is that of a mixture of equal volumes of solutions of the two substances, each at 2.0×10^{-4} M before mixing. The solvent is dimethylformamide and the quartz cell path length is 5 mm.

N-CH_3TPP ligand to *N*-methyldeuteroporphyrin, the reverse reaction utilizing chloro-*N*-methyldeuteroporphinatocobalt(II) and the free base H*N*-CH_3TPP was observed. Again, only the additive spectrum is observed after 1 week duration at 25 °C (Figure 5). From a comparison of the additive spectra obtained from these two experiments, it is evident that exchange to form a random mixture of products could readily be observed. Similar experiments were run with the zinc(II) complexes and free bases of both porphyrins. Both the cobalt(II) and zinc(II) experiments were carried out in CH_2Cl_2, CH_3CN, and DMF. In view of the recent work of Hambright on replacement of cadmium(II) in Cd(*N*-CH_3TPP)$^+$ by copper(II),[7] we also performed an experiment in which Cd(*N*-CH_3TPP)Cl was mixed with *N*-methyldeuteroporphyrin IX in DMF. Less than 20% exchange was evident after 7 days at 25 °C.

Attempts to cause dissociation of the metal atom from *N*-CH_3TPP by using a ligand which forms very stable metal complexes of zinc(II), cobalt(II), and cadmium(II) were made

Table VIII. Rate Constants for the Ni(II)-Catalyzed Replacement of Cd(II) in Cd(N-CH_3TPP)$^+$ by Cu(II)[a]

k_{obsd}, min^{-1} [b]	[Ni^{2+}], M	[H_2O], M	[Cu^{2+}], M	k^{3rd},[c] M^{-2} min^{-1}
0.031	0.066	0.46	6.6×10^{-5}	1.02
0.029	0.066	0.46	6.6×10^{-5}	0.96
0.030	0.066	0.46	3.3×10^{-5}	0.99
0.033	0.033[d]	0.92	6.6×10^{-5}	1.09
0.016	0.033[e]	0.46	6.6×10^{-5}	1.05
0.058	0.066	0.92	6.6×10^{-5}	0.96
0.056	0.066	0.92	6.6×10^{-5}	0.92

[a] At these concentrations, formation of CuN-CH_3TPP^+ as product is greater than 10 times faster than formation of NiN-CH_3TPP^+. [b] [Cd(N-CH_3TPP)$^+$] = 3×10^{-6} or 6×10^{-6}, with [Cu^{2+}] as least tenfold in excess for each run. T = 25.5 °C. [c] The rate constant for: rate = k^{3rd}[Ni^{2+}][H_2O][Cd(N-CH_3TPP)$^+$]. [d] I = 0.22 with 0.12 M (Bu_4N)(CF_3SO_3). [e] I = 0.20 with 0.10 M (Bu_4N)(CF_3SO_3).

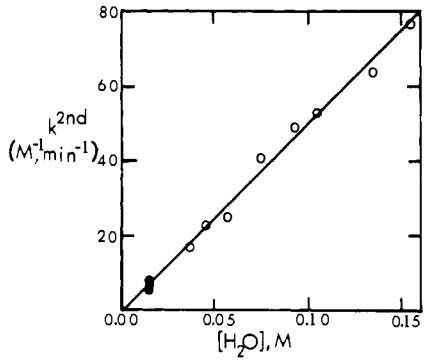

Figure 6. Second-order rate constants for the replacement of Cd(II) in Cd(N-CH_3TPP)$^+$ by Cu(II) in DMF at 25 °C (I = 0.36 M, (Bu_4N)BF_4; [Cu(BF_4)$_2$] = 4.56×10^{-3} M, [Cd(N-CH_3TPP)Cl] from 1.0×10^{-5} M to 1.0×10^{-4} M). Solid circles are rates for solutions to which no water was added (0.010 M H_2O in distilled DMF by GC analysis, 0.005 M H_2O contributed by Cu(BF_4)$_2$ by EDTA titration).

using acetylacetone, dialkylamines, and ethylenediamine. Solutions of acetylacetone (1.7 M) in acetonitrile did not cause dissociation after 24 h at 25 °C. Diethylamine and di-n-butylamine (in CH_3CN and DMF) did not cause dissociation at 25 °C after 1 week. Demethylation reactions are observed when solutions of the N-CH_3TPP complexes and dialkylamines in acetonitrile are refluxed, but isosbestic points observed throughout the reaction indicate that very little, if any, dissociation occurs.[13] These N-methylporphyrin complexes are not as inert as corresponding nonmethylated porphyrin complexes, however, since 1.0 M ethylenediamine in DMF at 25 °C causes demetalation of the Zn(II) and Cd(II) complexes on mixing and demetalation of Co(II) with a half-life of 36 s (porphyrin complexes at 1.0×10^{-4} M). The ZnTPP and CoTPP complexes are stable in solutions of 1.0 M ethylenediamine for days. From the results of the porphyrin exchange experiments and the rapid reaction with ethylenediamine, we presume that the ethylenediamine demetalation mechanism is associative.

The Copper–Cadmium Replacement Reaction

These results may be applied to the proposed mechanism of metal ion exchange for Cu(II) replacing Cd(II) in Cd(N-CH_3TPP)$^+$.[7] The reported kinetic data[7] for the reaction:

$$Cu^{2+} + Cd(N\text{-}CH_3TPP)^+ \rightarrow Cu(N\text{-}CH_3TPP)^+ + Cd^{2+}$$

in DMF at 25 °C result in a rate law first order in Cu^{2+} and in Cd(N-CH_3TPP)$^+$ and a second-order rate constant of 25.7 M^{-1} min^{-1}. the dissociative mechanism for the Cu(II)–Cd(II) replacement reaction may be written:

$$Cd(N\text{-}CH_3TPP)^+ \underset{k_{-1}}{\overset{k_1}{\rightleftharpoons}} Cd^{2+} + N\text{-}CH_3TPP^-$$

$$Cu^{2+} + N\text{-}CH_3TPP^- \xrightarrow{k_2} Cu(N\text{-}CH_3TPP)^+$$

A more likely form[35] of the mechanism would be:

$$Cd(N\text{-}CH_3TPP)^+ \rightleftharpoons Cd^{2+} + N\text{-}CH_3TPP^-$$

$$N\text{-}CH_3TPP^- + H^+ \rightleftharpoons HN\text{-}CH_3TPP$$

$$Cu^{2+} + HN\text{-}CH_3TPP \xrightarrow{k_2'} Cu(N\text{-}CH_3TPP)^+ + H^+$$

which involves the reaction of Cu^{2+} with the neutral free base N-methylporphyrin. For this scheme to be consistent with the observed rate law, the rate-determining step would be the last one, involving Cu^{2+}, but the slow exchange of Cd(II) from Cd(N-CH_3TPP)$^+$ to N-methyldeuteroporphyrin discussed above is inconsistent with this scheme. In addition, the lack of reaction of Cd(N-CH_3TPP)$^+$ in the presence of 1.0 M diethylamine demonstrates that either (1) the dissociation of Cd(N-CH_3TPP)$^+$ is too slow to justify this scheme or (2) the stability constant of Cd(N-CH_3TPP)$^+$ is very high ($>2.0 \times 10^{10}$, assuming that 3% dissociation could go unobserved and using the stability constant of Cd($(CH_3)_2NH)_4^{2+}$ which is 2.0×10^7).[36] In either case, the direct dissociation mechanism is unreasonable. The replacement of Cd(II) by Cu(II) in Cd(N-CH_3TPP)Cl, therefore, does not involve simple dissociation of Cd(II) from Cd(N-CH_3TPP)$^+$ as a first step.

A water-dependent reaction path, presumably involving displacement of Cd(II) before attack of Cu(II), is available for this reaction:

$$Cu^{2+} + H_2O \rightleftharpoons CuOH^+ + H^+$$

$$Cd(N\text{-}CH_3TPP)^+ + H^+ \rightleftharpoons Cd^{2+} + HN\text{-}CH_3TPP$$

$$Cu^{2+} + HN\text{-}CH_3TPP \rightarrow Cu(N\text{-}CH_3TPP)^+$$

Although we have shown that simple dissociation of Cd(N-CH_3TPP)$^+$ is not feasible in light of the overall rate for Cu(II) displacement of Cd(II), this associative reaction involving H$^+$ (from H_2O) displacement of Cd(II) could be significant. Hence, we studied the rate of reaction of Cd(N-CH_3TPP)Cl with Cu(BF_4)$_2$ in DMF (I = 0.36 M, (Bu_4N)BF_4, 25 °C) as a function of water concentration. The concentration of water in the solution after distillation of the DMF and drying of Cu(BF_4)$_2$ was determined to be 0.015 M (0.010 M from the DMF itself and 0.005 M contributed by the dissolved Cu(BF_4)$_2$). As is evident from Figure 6, the reaction is first order in H_2O with a third-order rate constant of 490 M^{-2} min^{-1} and shows no evidence of a water-independent path. Two tests of this scheme were made. To ensure that water alone did not cause a direct dissociation by a mechanism such as:

$$H_2O\text{-}Cd(N\text{-}CH_3TPP)^+ \rightleftharpoons H^+ + HO\text{-}Cd(N\text{-}CH_3TPP) \rightleftharpoons HN\text{-}CH_3TPP + CdOH^+$$

the Cd(N-CH_3TPP)–N-methyldeuteroporphyrin exchange reaction was run with water added. Even with [H_2O] as high as 5.5 M, the exchange rate was very slow ($t_{1/2}$ = 107 h at 25 °C). This reaction goes completely to the N-methyldeuteroporphinatocadmium(II) complex, as would be expected since

the pyrrole-substituted *N*-methylporphyrins are much more basic than *N*-methyltetraphenylporphyrin.[8,37] The second test involved the use of another metal ion which causes hydrolysis, but which still allows Cu^{2+} to react with the free *N*-methylporphyrin. Nickel(II) was chosen because it reacts much more slowly with H*N*-CH_3TPP than does Cu(II). Since Ni(II) causes hydrolysis to a much smaller extent than does Cu(II),[36] a large excess of Ni(II) was employed. As is evident from Table VIII, the observed exchange rate in the presence of a large excess of Ni(II) relative to Cu(II) is first order in Ni(II), H_2O, and Cd(*N*-CH_3TPP)$^+$ and independent of the concentration of Cu(II).

An observation which is troublesome with respect to the proposed mechanism involving acid-catalyzed dissociation of the cadmium porphyrin complex is that added Cd^{2+} does not inhibit this reaction, a fact supporting an associative mechanism involving attack of Cu^{2+} on the same side of the porphyrin ligand as the bound Cd(II) atom.[7] The highest ratio of Cd^{2+} to Cu^{2+} studied, however, was about 60. Thus, if the rate of incorporation of Cu^{2+} into the dissociated *N*-methylporphyrin ligand is over two orders of magnitude greater than the Cd^{2+} incorporation rate, inhibition would not be evident. Until the kinetic data for these metal incorporation reactions become available, the lack of inhibition cannot be considered to be definitive support for an associative mechanism.

These kinetic results on Cd(II) exchange from *N*-methyltetraphenylporphyrin and the dependence of the rate of Cu(II) replacement of Cd(II) on water concentration lead to the conclusion that there is no compelling evidence for a mechanism involving electrophilic attack of a metal ion on the side of a porphyrin occupied by a bound metal ion. Instead, a mechanism involving predissociation of Cd(*N*-CH_3TPP)$^+$ due to associative attack by H^+ is proposed. It should be noted that most metal exchange reactions of porphyrins that have been studied[3] involve porphyrins that are readily acid dissociated (Zn(II), Cd(II), Hg(II), and Pb(II) complexes), and further study of these reactions is warranted.

Acknowledgment. We appreciate the technical assistance of Ms. Felice Barrett. D.K.L. wishes to thank the donors of the Petroleum Research Fund, administered by the American Chemical Society, for partial support of this work. Computing funds were supplied by Colorado State University and the Colorado State University Computing Center.

Supplementary Material Available: A listing of observed and calculated structure factor amplitudes (24 pages). Ordering information is given on any current masthead page.

References and Notes

(1) Address correspondence for this author to: Department of Chemistry, Hunter College, CUNY, 695 Park Ave., New York, N.Y. 10021.
(2) (a) S. Rubin, A. W. Frenkel, M. B. Allen, and P. Nakinsky, *J. Am. Chem. Soc.*, **64**, 2297 (1942). (b) S. Rubin, A. W. Frenkel, and M. D. Kamer, *J. Phys. Chem.*, **46**, 710 (1942).
(3) C. Grant, Jr., and P. Hambright, *J. Am. Chem. Soc.*, **91**, 4195 (1969).
(4) N. Ashelford and D. P. Mellon, *Aust. J. Sci. Res., Ser. A*, **5**, 784 (1952).
(5) O. P. Anderson and D. K. Lavallee, *J. Am. Chem. Soc.*, **98**, 4670 (1976); **99**, 1404 (1977).
(6) O. P. Anderson and D. K. Lavallee, *Inorg. Chem.*, **16**, 1634 (1977).
(7) C. Stinson and P. Hambright, *J. Am. Chem. Soc.*, **99**, 2357 (1977).
(8) D. K. Lavallee and A. E. Gebala, *Inorg. Chem.*, **13**, 2004 (1974).
(9) D. K. Lavallee and M. J. Bain, *Inorg. Chem.*, **15**, 2090 (1976).
(10) D. D. Perrin, W. L. F. Armarego, and D. R. Perrin, "Purification of Laboratory Chemicals", Pergamon Press, London, 1966.
(11) D. K. Lavallee, *Bioinorg. Chem.*, **6**, 291 (1976).
(12) D. K. Lavallee, *Inorg. Chem.*, **15**, 691 (1976).
(13) D. K. Lavallee, *Inorg. Chem.*, **16**, 955 (1977).
(14) "International Tables for X-Ray Crystallography", Vol. I, Kynoch Press, Birmingham, England, 1969.
(15) Using the automated routines incorporated in the Enraf-Nonius diffractometer package.
(16) P. W. R. Corfield, R. J. Doedens, and J. A. Ibers, *Inorg. Chem.*, **6**, 197 (1967).
(17) O. P. Anderson, A. B. Packard, and M. Wicholas, *Inorg. Chem.*, **15**, 1613 (1976).
(18) Single-crystal x-ray fluorescence analysis was kindly performed by Dr. C. J. Weschler, Bell Telephone Laboratories, Holmdel, N.J.
(19) "International Tables for X-Ray Crystallography", Vol. IV, Kynoch Press, Birmingham, England, 1974.
(20) R. F. Stewart, E. R. Davidson, and W. T. Simpson, *J. Chem. Phys.*, **42**, 3175 (1965).
(21) The following programs were used in this structure determination: Zalkin's FORDAP Fourier program; Ibers' NUCLS, a group least-squares version of the Busing–Levy ORFLS program; Ibers' CELREF for least-squares refinement of cell parameters; ORFFE, Busing and Levy's function and error program; ORTEP, Johnson's thermal ellipsoid plotting program. The program for data reduction and Lp correction was written locally for the CDC 6400 computer.
(22) P. R. Hoffman, T. Yoshida, T. Okano, S. Otsuka, and J. A. Ibers, *Inorg. Chem.*, **15**, 2462 (1976).
(23) P. Eisenberg and J. A. Ibers, *Inorg. Chem.*, **4**, 773 (1965).
(24) W. P. Scheidt and W. Dow, *J. Am. Chem. Soc.*, **99**, 1101 (1977), and references therein.
(25) D. M. Collins and J. L. Hoard, *J. Am. Chem. Soc.*, **92**, 3761 (1970).
(26) E. B. Fleischer, C. K. Miller, and L. E. Webb, *J. Am. Chem. Soc.*, **86**, 2342 (1964).
(27) D. L. Cullen and E. F. Meyer, Jr., *Acta Crystallogr., Sect. B*, **32**, 2259 (1976).
(28) T. Kobayashi, T. Ashida, N. Uyeda, E. Suito, and M. Kakudo, *Bull. Chem. Soc. Jpn.*, **44**, 2095 (1971).
(29) D. E. Goldberg and K. M. Thomas, *J. Am. Chem. Soc.*, **98**, 913 (1976).
(30) The term "planar" is used here simply to denote a nonmethylated porphyrin.
(31) W. R. Scheidt and J. A. Ramanuja, *Inorg. Chem.*, **14**, 2643 (1975).
(32) H. P. Bennetto and E. F. Caldin, *J. Chem. Soc. A*, 2191, 2198, and 2207 (1971).
(33) R. G. Wilkins, "The Study of Kinetics and Mechanism of Reactions of Transition Metal Complexes", Allyn and Bacon, Boston, Mass., 1974, p 222.
(34) M. Eigen, *Pure Appl. Chem.*, **6**, 105 (1963).
(35) The monoanionic form of porphyrin is a strongly basic species, not being observed in the presence of even trace amounts of water.
(36) L. G. Sillen and A. E. Martell, *Chem. Soc. Spec. Publ.*, **No. 25** (1971). The stability constants given therein are for aqueous solutions rather than dimethylformamide solutions.
(37) A Neuberger and J. J. Scott, *Proc. R. Soc. London*, **213**, 307 (1952).